

## Experimental Study for Synthetic Aperture Telescope Using Formation Flying Micro-satellites for High-frequency and High-resolution GEO Remote Sensing

Ryo Suzumoto, Satoshi Ikari  
The University of Tokyo  
7-3-1 Hongo, Bunkyo-ku, Tokyo 113-8656, Japan; +81-3-5841-6631  
suzumoto@space.t.u-tokyo.ac.jp

Norihide Miyamura  
Meisei University  
2-1-1 Hodokubo, Hino, Tokyo 191-8506, Japan; +81-42-591-5895  
norihide.miyamura@meisei-u.ac.jp

Shinichi Nakasuka  
The University of Tokyo  
nakasuka@space.t.u-tokyo.ac.jp

### ABSTRACT

Earth remote sensing from geostationary orbit (GEO) realizes high time resolution that is essential for disaster monitoring; however, the spatial resolution is commonly worse than observation from low Earth orbit. In order to achieve high-resolution and high-frequency GEO remote sensing, we have proposed a “Formation Flying Synthetic Aperture Telescope (FFSAT)” with multiple micro-satellites. The FFSAT can improve the spatial resolution by using the technique of a synthetic aperture, and therefore the relative positions and attitudes between the optical units of each satellite must be controlled with an accuracy better than 1/10 of the observation wavelength. In order to verify feasibility of such highly accurate control, the characteristics of sensors and actuators which are essential for an ultra-high-accuracy formation flying were numerically modeled. We consider control laws for keeping the relative position and attitude of the  $\mu$ m-class formation flying using the high-precision simulator built on the numerical models. In addition, the cooperative control of the piezo stages and the thrusters is studied to reduce the fuel consumption of the FFSAT system. The simulation results made the FFSAT mission more feasible.

### INTRODUCTION

Disaster monitoring using Earth observation satellites is a valuable information source to grasp wide-area ground situations at one time. Spatial resolution (image resolution) and observation frequency (temporal resolution) are important factors for practical applications<sup>1</sup>. Geostationary orbit (GEO) remote sensing, which utilizes Earth observation satellites positioned in GEO, can realize high-frequency observation even to the level of several minute interval such as the case of “Himawari”<sup>2</sup>. However, because of their high altitude, it has the disadvantage that it is difficult to obtain high spatial resolution compared to observation from low Earth orbit (LEO). In order to improve the resolution, only one solution is to increase the aperture size of the optical system. However due to restrictions for a size of a launch vehicle and development cost of such large satellites, it would be very difficult to put a huge optical system in GEO. Although there is an approach to eliminate the need for large structures by manufacturing and deploying boom structure in space<sup>3</sup>, there is a physical upper limit to the aperture diameter. As an

alternative way to improve the resolution without using a huge structure, “a synthetic aperture telescope” has been studied<sup>4</sup>. The method obtains a virtual large aperture by precisely arranging small sub-apertures that are interferometrically combined to achieve a resolution comparable to a primary aperture whose size is equivalent to the entire distributed array size. As a space telescope, a synthetic aperture telescope constructed by satellite formation flying such as TPF-I mission<sup>5</sup> has been proposed. It can realize a large aperture which is not comparable to that of a single satellite and can attain a high resolution which has never been achieved before. However, due to the high required control accuracy and development cost, this mission has not been realized until now.

As a method to realize high-resolution and high-frequency observation for the GEO remote sensing, we have proposed to use a synthetic aperture telescope comprised of multiple formation flying micro-satellites which are precisely controlled in position and attitude. We named it “Formation Flying Synthetic Aperture

Telescope (FFSAT)”. In Figure 1, six mirror satellites form a virtual large mirror, which is focused on an imaging satellite. Furthermore, we have considered the Australian forest fire monitoring mission as the first practical application of the FFSAT. In the past, satellites Terra and Aqua equipped with NASA’s visible/infrared radiometer MODIS achieved 1 km ground sample distance (GSD) from the altitude of 705 km, with the observation frequency of one to two days<sup>6</sup>. On the other hand, FFSAT preliminarily designed by the authors<sup>7</sup> is expected to achieve both high-resolution observation of 30 m GSD and high-frequency observation on the order of 10 minutes in infrared rays (as shown in Table 1).

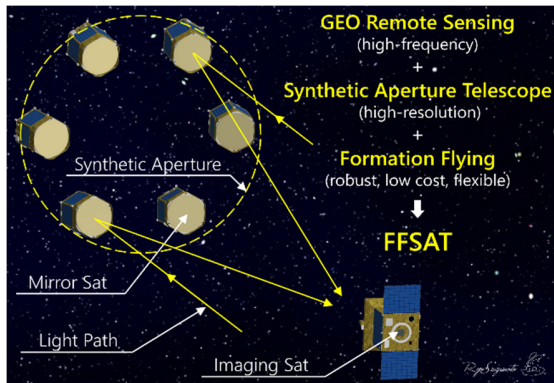


**Figure 1: Concept image of the FFSAT**

**Table 1: Requirements of the FFSAT for the forest fire monitoring mission**

	Unit	Value
GSD	m	Normal
Field of view	km×km	1,000 × 1,000
Observation frequency	min	10
Orbital altitude	km	35,786 (GEO)
Observation wavelength	μm	4 (infrared)
Focal length	m	21.5
Synthetic aperture diameter	m	5.82
Required piston control accuracy	μm	0.40
Required tilt control accuracy	μrad	0.42

The FFSAT can achieve both high-resolution observation and high-frequency observation. However, realization of FFSAT requires determining and controlling the relative positions and attitudes of formation flying satellites with an accuracy better than 1/10 of the observation wavelength (e.g., in the case of near infrared ray, 0.1 μm order)<sup>4</sup>, which is extremely high-accuracy as compared with the past studies on

formation flying. Figure 2 shows the relative position control accuracy of formation flying missions and related technologies. The area surrounded by the blue dashed line is already demonstrated on orbit. As for a nano- and micro-satellite formation flying, CanX-4&5 mission have succeeded in formation control to an accuracy of 1 m<sup>8</sup>. In recent years, formation flying mission projects with cm-class accuracy such as mDOT<sup>9</sup> are proposed, which are included in the area surrounded by the red dashed line. By contrast, the required control accuracy of the FFSAT is 0.1 μm order, which is incomparably high as shown in Figure 2. Figure 3 summarizes the accuracy and operation range of sensors and actuators, which are commercial off-the-shelf (COTS) products and small enough to be installed in micro-satellites. High-precision thrusters such as cold gas thrusters and colloid thrusters are being developed<sup>10</sup>, but they do not reach the required accuracy of the FFSAT. Besides, fuel consumption tends to be high when thrusters are used for fine control. To overcome the accuracy limits of thrusters, more precise device like piezo stages can be useful. ASTERIA<sup>11</sup> has achieved great pointing accuracy of 2.4 μrad/20 minutes (1σ) using a satellite attitude control system in combination with piezo stages. A deformable mirror which can drive a mirror surface with an accuracy of less than the wavelength order is widely used in the field of optical compensation. DeMi<sup>12</sup> was launched in 2020 to demonstrate a deformable mirror on orbit. Highly accurate relative position and attitude estimation among satellites can be achieved by accurate measurement of the distance between multiple points of satellites. However, there is no absolute distance meter in the range marked “Gap” in Figure 3.

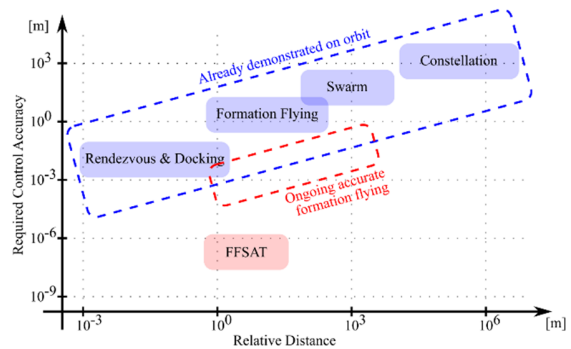


**Figure 2: Comparison with related technologies**

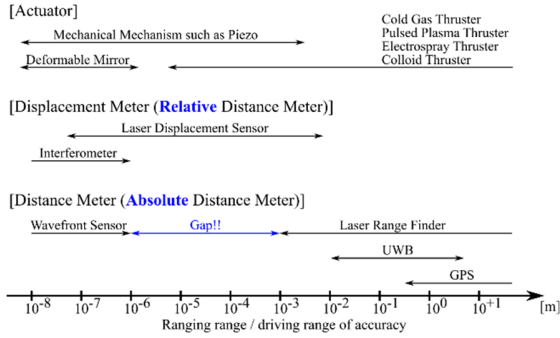


**Figure 3: Accuracy and operation range of sensors and actuators available for micro-satellites**

We have already conducted some studies to realize formation flying with an accuracy of 1/10 of the observation wavelength. In order to fill the gap of the absolute distance meter shown in Figure 3 and construct an ultra-high-accuracy formation flying for the FFSAT, we have proposed a method called “PSF optimization method”<sup>7</sup>. In this method, a captured point light source image by the FFSAT is optimized while observing the relative position and attitude displacement between satellites with high-precision displacement sensors. Consequently, even if the absolute distance between satellites cannot be measured with high accuracy, the algorithm to construct an ultra-high-accuracy formation flying that can obtain an effective image was shown. In addition, by using deformable mirrors, we have proposed methods to improve the image quality at the edge of view, and to change the direction of the telescope without moving the center of gravity of the formation flying satellites<sup>13</sup>. However, in order to effectively use these methods and to make observations, it is necessary to keep the constructed or constructing formation with ultra-high accuracy. Therefore, a control law using multi-stage actuators composed of thrusters, piezo stages, and deformable mirrors is required.

In order to construct a control law of formation flying with an accuracy of  $\mu\text{m}$  order or less, a numerical simulator with the equivalent precision is required. For this purpose, we have created numerical models of the components essential for the ultra-high-accuracy formation flying by using the results of hardware experiments. In order to confirm the validity of the numerical models, the hardware experiments were emulated by software simulations. For the components that are difficult to conduct experiments, we have modeled them by referring to the verification results of existing ones. Based on these numerical models, we have constructed a high-precision simulator for the FFSAT system<sup>14</sup>. In this paper, we consider the control laws of the relative position and attitude of the  $\mu\text{m}$ -class

formation flying using the high-precision simulator built on the numerical models. Based on observations with high-precision laser displacement sensors (LDSs), the relative position and attitude among satellites could be controlled with  $\mu\text{m}$ -class accuracy using dual-stage actuators, which consist of cold gas thrusters and piezo stages. In addition, the cooperative control of the piezo stages and the thrusters is studied to reduce the fuel consumption of the FFSAT system. Please note that adaptive optics and deformable mirrors will be used for 0.1  $\mu\text{m}$ -class control, but we do not deal with that in this paper.

## MODELING AND SIMULATOR

We have already worked on the numerical modeling of components. For details of their results, we refer to our previous work<sup>14</sup>. Here we describe the outline of the modeling and the high-precision simulator for constructing the control laws in the next section.

### Modeling of components

Numerical modeling of LDSs and piezo stages was performed using the experimental setups shown in Figures 4 and 5. For the LDSs, the measurement accuracy, the measurement frequency, and the measurement time delay were modeled. For the piezo stages, the time delay, control frequency, and hysteresis were modeled. In addition, it was shown that  $\mu\text{m}$ -class control is possible by 3-axis experimental setups as shown in Figure 6. In addition, cold gas thrusters were numerically modeled from the required noise level of the thruster used in ESA's LISA Pathfinder<sup>15</sup>, and a simple model was also created for the absolute attitude sensor consisting of star trackers (STT) and fiber-optic gyroscopes (FOG).

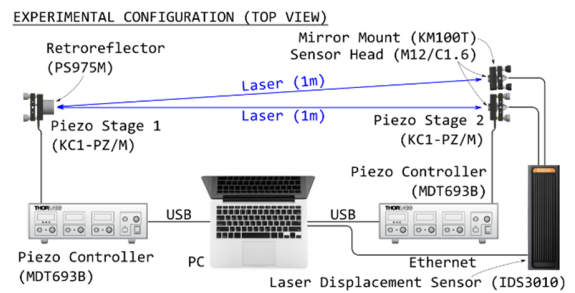


**Figure 4: Configuration for single-axis experiment<sup>14</sup>**

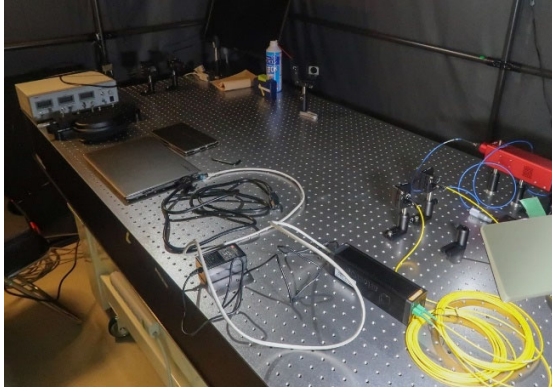


Figure 5: Configuration for single-axis experiment

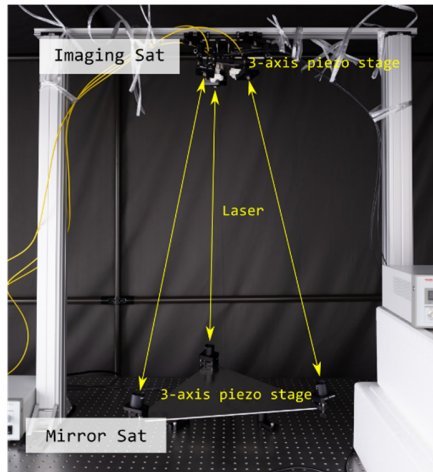


Figure 6: Configuration for 3-axis experiment<sup>14</sup>

### High-precision simulator for the FFSAT system

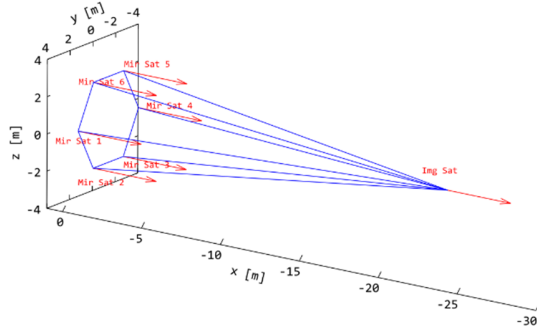
In the FFSAT currently under consideration, there are seven satellites, and six axes of each position and attitude must be controlled with  $\mu\text{m}$ -class accuracy. Therefore, a high-precision software simulator for the FFSAT system reflected the results of the numerical modeling was created. Then, in the next section, we will consider the control law of FFSAT using this simulator.

It is assumed that the STTs, the FOGs, the LDSs are installed as sensors, and the cold gas thrusters and the piezo stages are installed as actuators. A reaction wheel (RW) is not installed because it is considered that the micro-vibrations caused by RWs adversely affect highly accurate control. Table 2 shows the specifications of the simulation. Figure 8 shows the determination and control dynamics of FFSAT. In the case of the imaging satellite, only the absolute attitude with respect to Earth was controlled because the position of the imaging satellite is

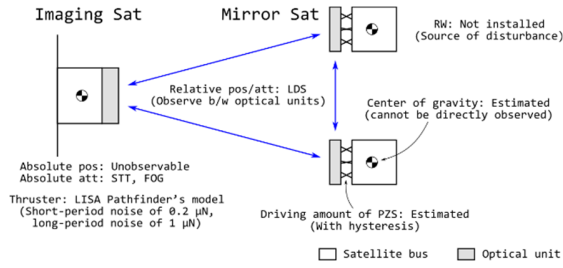
set as the origin of the formation coordinate and the absolute position of formation flying is not focused on in this simulation. All mirror satellites followed the imaging satellite to keep the relative position and attitude with respect to the imaging satellite. If the imaging satellite has a high control frequency and vibrates rapidly in a small width, it will be difficult for the mirror satellites to follow it. Accordingly, the control frequency of the imaging satellite was set low.

Table 2: Specifications of the simulation for keeping the formation of the FFSAT

SATELLITE	
Number	1 imaging satellite and 6 mirror satellites
Mass, Moment of inertia	50 kg-class. Use the value designed by the authors <sup>7</sup> . The values of the 6 mirror satellites were given a variation of 0.1 %
ORBIT	
Coordinate	Local-Vertical-Local-Horizontal (LVLH) frame
Initial orbit	GEO at an east longitude of 140°
Formation	See Figure 7. The origin is GEO at an east longitude of 140°. Satellites are placed at the intersection of the blue lines, and the red arrows indicate the satellites' z axis.
Propagation	RK4 with the time interval of 0.1 s in ECI.
ORBITAL DISTURBANCE	
Geopotential	Up to third order
Third bodies	Sun, Moon
COMPONENT	
LDSs	The displacements can be measured with 100 nm accuracy ( $1\sigma$ ), and the positions of the laser receiving point can be measured with 1 $\mu\text{m}$ accuracy ( $1\sigma$ ).
STTs & FOGs	Absolute attitude estimation accuracy of 10 $\mu\text{rad}$ ( $1\sigma$ ). The noise model was white Gaussian noise.
Piezo stages	Numerical model constructed by the authors <sup>14</sup> . 0.1 second response delay. Maximum stroke was 10 $\mu\text{m}$ and 10 $\mu\text{rad}$ .
Thrusters	Numerical model constructed by the authors <sup>14</sup> . Maximum thrust is 20 $\mu\text{N}$ . All satellites had 12 control thrusters, 2 on each of 6 planes ( $\pm x, y, z$ ), for highly accurate position and attitude control. In addition, there is one constant thruster to cancel the relative gravity disturbance derived from Hill's equation.
RWs	Not installed
CONTROL	
Control law	The mirror satellites follow the imaging satellite.
Frequency	1/10 Hz for the imaging satellite, 10 Hz for the thrusters of the mirror satellites, and 20 Hz for the piezo stages of the mirror satellites.



**Figure 7: Initial formation of the FFSAT in LVLH frame**



**Figure 8: Dynamics of the FFSAT**

## CONTROL LAWS AND SIMULATION RESULTS

We describe the control laws of FFSAT using the simulator developed in the previous section. The important thing here is to reduce fuel consumption while achieving high control accuracy of the relative position and attitude.

### Simple PID control (non-cooperative control)

First of all, a simple PID control was considered. Since the dynamics of FFSAT is as shown in Figure 8, the relative position and attitude errors of the optical units of the mirror satellites can be obtained by the observation of LDSs. Furthermore, the relative position and attitude errors of the center of gravity of the mirror satellites can be estimated from the observation of LDSs and the control input to the piezo stages. Let  $e_{\text{obs}}^{\text{opt}}$  be the observed errors of the optical unit of the mirror satellite by using the LDSs and  $e_{\text{est}}^{\text{cg}}$  be the estimated errors of the center of gravity of the mirror satellite.  $e_{\text{est}}^{\text{cg}}$  is estimated from  $e_{\text{obs}}^{\text{opt}}$  and the control input to the piezo stages. Then, the control input to the control thrusters  $u^{\text{thr}}$  and that of the piezo stages  $u^{\text{pzs}}$  are expressed as follows:

$$\begin{cases} u^{\text{pzs}} = \text{PID}(e_{\text{obs}}^{\text{opt}}) \\ u^{\text{thr}} = \text{PID}(e_{\text{est}}^{\text{cg}}) \end{cases} \quad (1)$$

In this control law, the thrusters and piezo stages are not controlled cooperatively, but are controlled independently. The gain of PID control was set to minimize the control errors.

Figures 10 and 10 show simulation results. From the top figure, the position errors of the mirror satellites with respect to the imaging satellite, the attitude errors of the mirror satellites with respect to the imaging satellite, absolute attitude error of the imaging satellite, the control history of control thrusters of the mirror satellite 2, and that of control thrusters of the imaging satellite are shown. In the control error graphs, the solid lines, broken lines, and dash-dot lines represent the  $x$ ,  $y$ , and  $z$  axes, respectively. At the beginning of the simulation, only the thrusters were used, and the piezo stages were driven 10 minutes after the start of the simulation. By using high-precision thrusters and piezo stages, the relative position control accuracy of  $0.24 \mu\text{m}$  and relative attitude control accuracy of  $0.23 \mu\text{rad}$  ( $3\sigma$ ) were achieved. It was found that the  $\mu\text{-class}$  control required to connect the control to adaptive optics using deformable mirrors can be achieved.

Since highly accurate control is required, the thrusters kept the relative position and attitude by continuously generating thrust from each side. The average impulse of the mirror satellite 2 at the simulation was approximately  $62 \mu\text{Ns/s}$ . In other words, the consumed fuel weight was about  $2.8 \text{ kg/year}$ , assuming cold gas thrusters with  $I_{\text{sp}}$  of 70 seconds. This is infeasible for missions of several years with micro-satellites, and a control law to reduce fuel is required.

### Deadband control

A control law to reduce fuel consumption was considered. The jitter of the control error, which is one of the causes of large fuel consumption, should be reduced. For the thrusters, PID control with deadband is performed, and the piezo stages are used for only  $\mu\text{-class}$  control. The thrust is not generated in the deadband of a control error less than a few  $\mu\text{m}$ . In this deadband control, the control inputs  $u$  are expressed as follows:

$$\begin{cases} u^{\text{pzs}} = \text{PID}(e_{\text{obs}}^{\text{opt}}) \\ u^{\text{thr}} = \begin{cases} 0 & \text{if } |e_{\text{est}}^{\text{cg}}| < w_{\text{db}} \\ \text{PID}(e_{\text{est}}^{\text{cg}}) & \text{otherwise} \end{cases} \end{cases} \quad (2)$$

where  $w_{\text{db}}$  is deadband width.



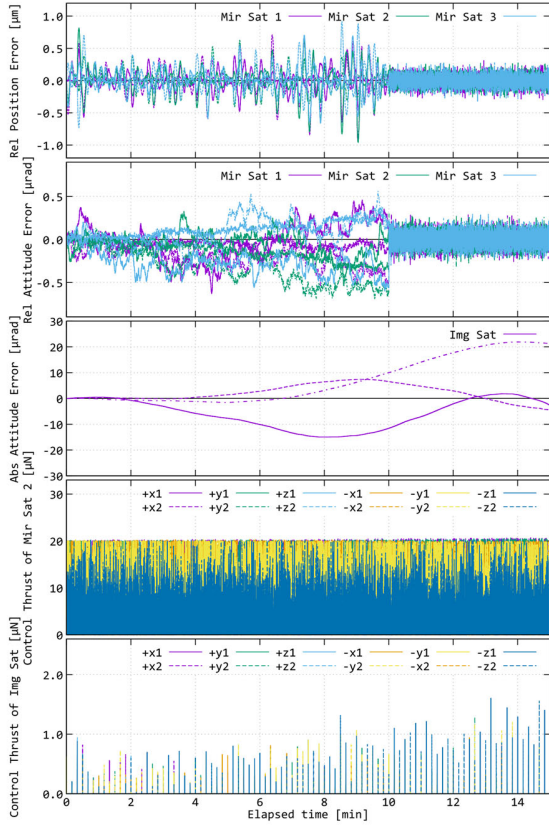


**Figure 10: Simulation results of the simple PID control**

The results of changing the deadband width and PID gains are shown in Figures 11 and 12, and a control history of one of the Pareto solutions is shown in Figures 13 and 14. As the required stroke of the piezo stages was increased, the fuel consumption decreased. However, it was found that when the stroke exceeded approximately 10  $\mu\text{m}$  and 5  $\mu\text{rad}$ , the fuel consumption did not decrease any further. When the deadband width is increased, the jitter of the thrusters is suppressed, and the fuel consumption is significantly reduced at first. After that, however, the control history becomes such that the control errors oscillate at the edge of the deadband, and the fuel consumption does not decrease.

Figures 13 and 14 show a simulation results of one of the Pareto solutions when the deadband width was 5.0  $\mu\text{m}$  and 5.0  $\mu\text{rad}$ , the average impulse of the thrusters was approximately 7.3  $\mu\text{Ns/s}$ , and the necessary stroke of the piezo stages was approximately 14  $\mu\text{m}$  and 19  $\mu\text{rad}$ . In Figure 13, the piezo stages were not driven. In Figure 14, they were driven and high control accuracy was achieved. The consumed fuel weight was about 0.34 kg/year, assuming cold gas thrusters with  $I_{sp}$  of 70 seconds.

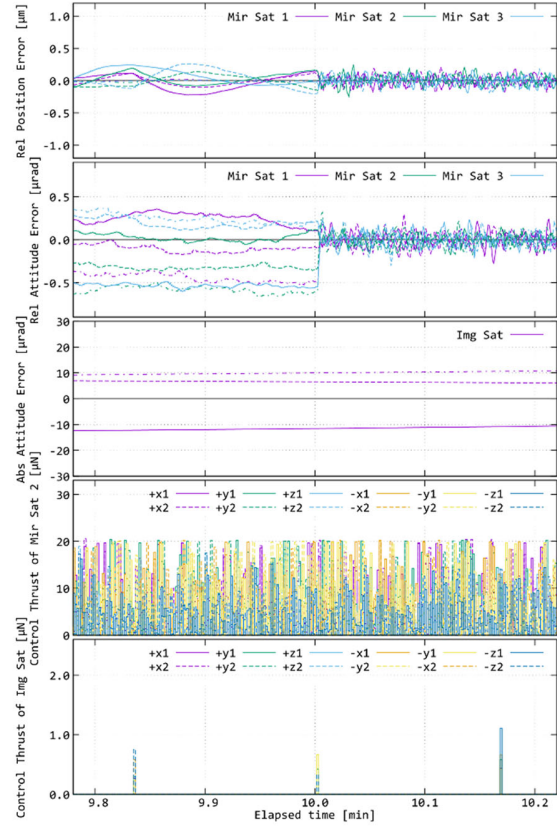


**Figure 10: Enlarged view of Figure 10**

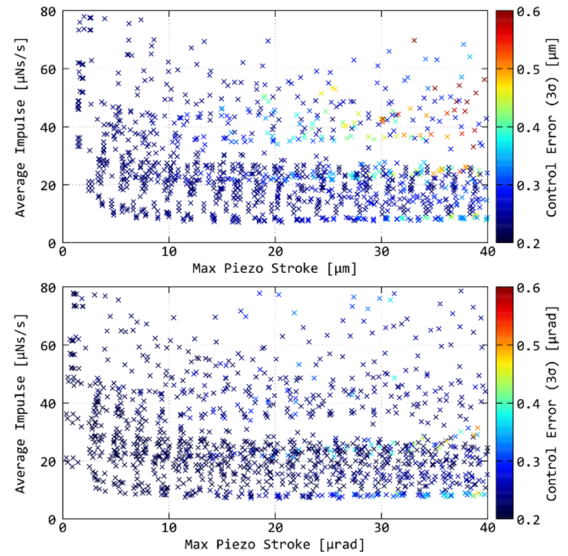


**Figure 11: Stroke required for the piezo stages and fuel consumption**

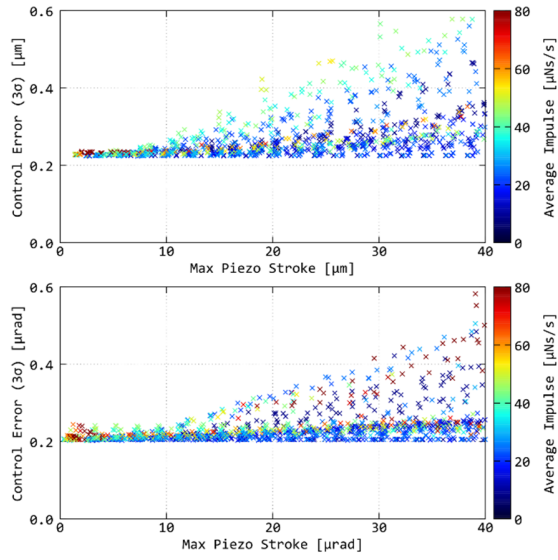


**Figure 12: Stroke required for the piezo stages and control accuracy**

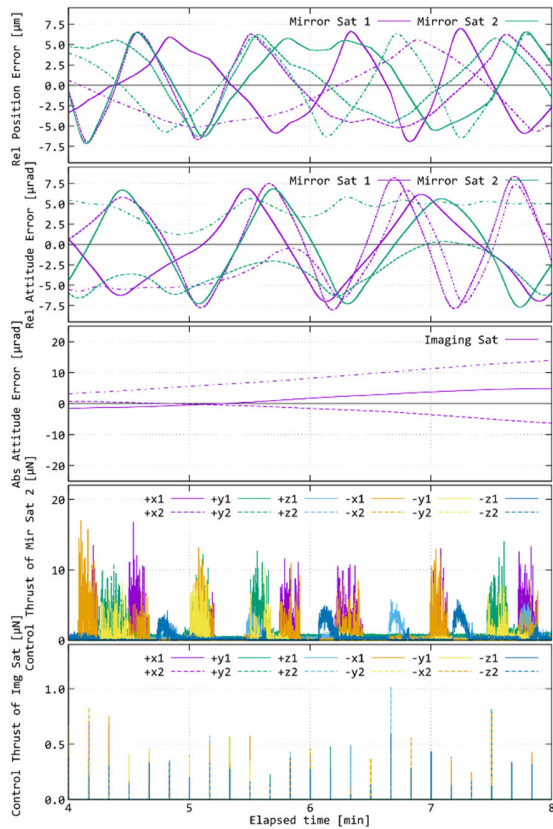


**Figure 13: Example of simulation results of the deadband control (only the thrusters)**

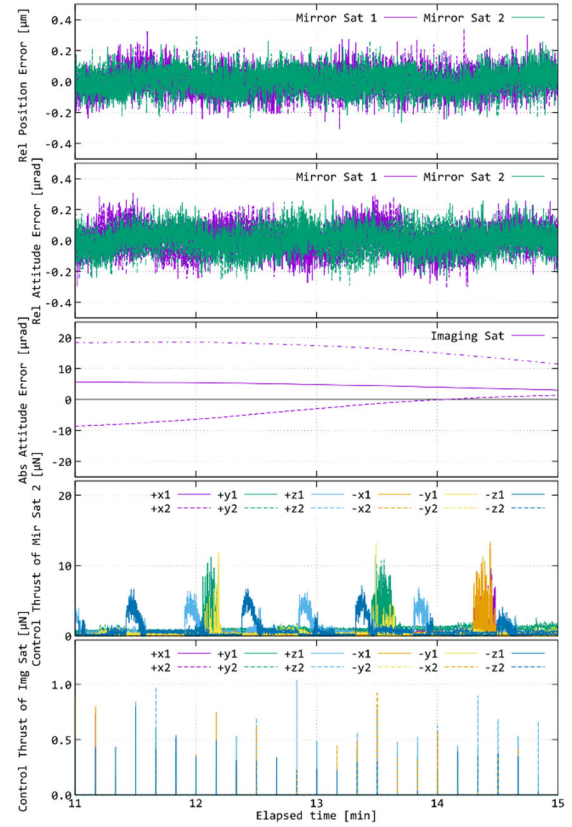


**Figure 14: Example of simulation results of the deadband control (the thrusters and piezo stages)**

#### Improved deadband control (proposed control law)

In order to extend the mission period, we propose a control law to further reduce the fuel consumption. When the control error exceeds the deadband at a certain speed, if P control is performed without any disturbances, it will reenter the deadband at the same speed. In such a control law, the time interval for going back and forth on both sides of the deadband does not become longer. In order to slowly return to the deadband, the D gain should be set large. However, if the D gain is too large, thrust in the direction opposite to the deadband will be generated, and fuel will be wasted.

Therefore, we proposed a control law that does not generate thrust when the error is decreasing toward the deadband. This control law is expressed as the following equation:

$$\begin{cases} \mathbf{u}^{\text{pzs}} = \text{PID}(\mathbf{e}_{\text{obs}}^{\text{opt}}) \\ \mathbf{u}^{\text{thr}} = \begin{cases} 0 & \text{if } |\mathbf{e}_{\text{est}}^{\text{cg}}| < \mathbf{w}_{\text{db}} \\ 0 & \text{if } f(\mathbf{e}_{\text{est}}^{\text{cg}}) < 0 \\ \text{PID}(\mathbf{e}_{\text{est}}^{\text{cg}}) & \text{otherwise} \end{cases} \end{cases} \quad (3)$$

where  $f$  is a function that determines that the control error  $|e_{\text{est}}^{\text{cg}}|$  tends to decrease. Since there is the estimation error of the control error, when strictly judging the decreasing trend of the control error, thrust will be generated even though the control error is decreasing, and fuel will be wasted. On the other hand, if the judgment is too lenient, the thrust will be decreased though the control error is increasing. In this simulation,  $f$  was defined as follows:

$$f(e_{\text{est}}^{\text{cg}}) = |e_{\text{est}}^{\text{cg}}(t)| - |e_{\text{est}}^{\text{cg}}(t - \Delta t_w)| \quad (4)$$

where  $t$  is time and  $\Delta t_w$  is a parameter.

The results of changing the deadband width and PID gains are shown in Figures 15 and 16. Figures 17 and 18 show a simulation results of one of the Pareto solutions when the deadband width was  $6.0 \mu\text{m}$  and  $6.0 \mu\text{rad}$ , the average impulse of the thrusters was approximately  $2.5 \mu\text{Ns/s}$ , and the necessary stroke of the piezo stages was approximately  $15 \mu\text{m}$  and  $16 \mu\text{rad}$ . In this result, the consumed fuel weight was about  $0.11 \text{ kg/year}$ , which was even less than the simple deadband control. With such a fuel consumption, it is considered possible to continue the FFSAT mission for several years.

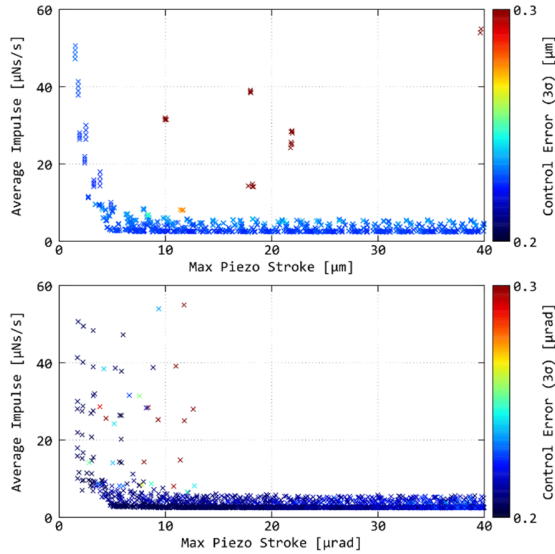


**Figure 15: Stroke required for the piezo stages and fuel consumption**

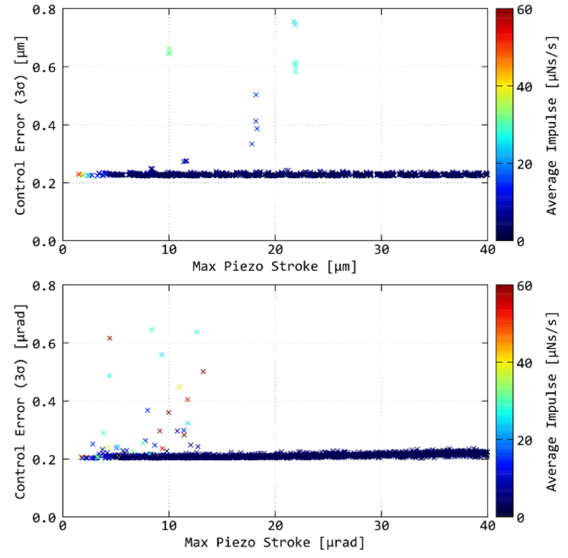


**Figure 16: Stroke required for the piezo stages and control accuracy**

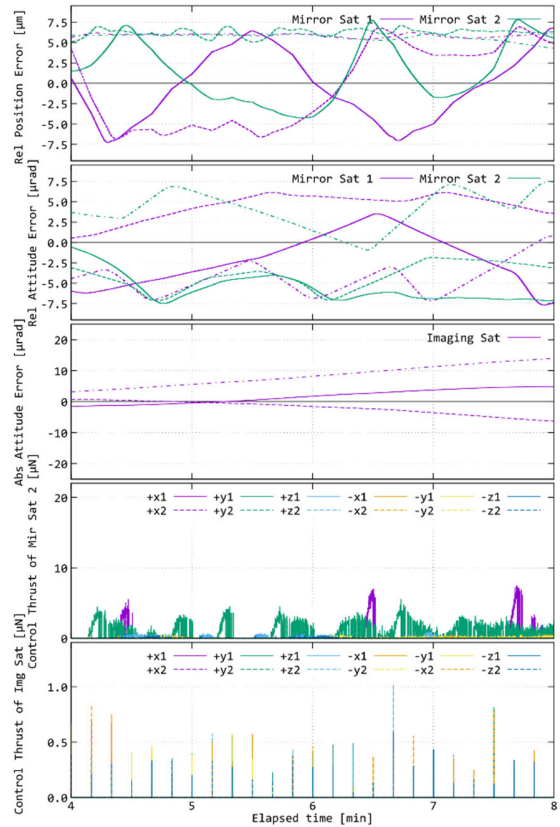


**Figure 17: Example of simulation results of the deadband control (only the thrusters)**



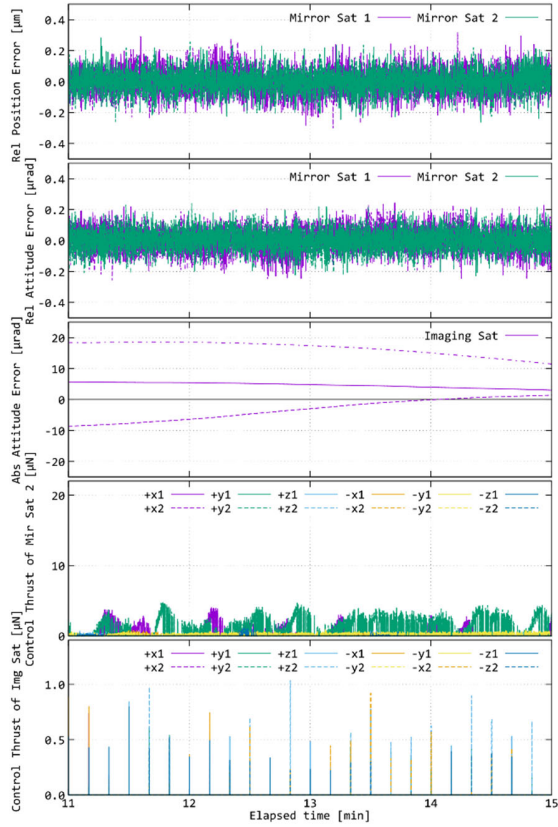


**Figure 18: Example of simulation results of the deadband control (the thrusters and piezo stages)**

### Comparison of the control laws

Table 3 summarizes the achieved control accuracy and fuel consumption of the three control laws shown so far. It can be seen that the proposed control law can significantly reduce fuel consumption, even though the control accuracy does not deteriorate compared to the other control laws. The proposed control law makes it possible to continue the FFSAT mission for several years. We think the residual control errors can be removed by adaptive optics using deformable mirrors.

**Table 3: Comparison of the control laws**

	Simple PID control	Deadband control	Proposed control
Control accuracy [μm]	0.24	0.27	0.25
Control accuracy [μrad]	0.23	0.24	0.21
Average impulse [μNs/s]	62	7.3	2.5

## CONCLUSION

In order to realize the “Formation Flying Synthetic Aperture Telescope (FFSAT)”, which can achieve high-resolution and high-frequency observation for the GEO remote sensing, the highly accurate formation keeping of μm-class was verified. In our previous work<sup>14</sup>, performance evaluation experiments using COTS components were conducted and the characteristics of the sensors and actuators which are essential for an ultra-high-accuracy formation flying were numerically modeled. In this paper, we consider control laws for keeping the relative position and attitude of the μm-class formation flying using the high-precision simulator built on the numerical models. Although the control accuracy better than μm order could be achieved by a simple non-cooperative control law using the high precision cold gas thrusters and piezo stages, the fuel consumption of the FFSAT system became infeasible to continue the FFSAT mission for several years. Therefore, we proposed a control law based on deadband control, and fuel consumption was greatly reduced. We think the residual control errors can be removed by adaptive optics using deformable mirrors. Although there are still other issues to consider such as thermal deformation, we believe that our series of studies have made the FFSAT mission more feasible.

In addition, the use of the FFSAT is not limited to GEO remote sensing. The FFSAT theoretically has no upper limit on its aperture diameter. The FFSAT has the possibility to realize much larger aperture diameter and to achieve much higher spatial resolution compared with conventional space telescopes. By applying the FFSAT to a astronomical observation telescope, an unprecedented observation such as a direct observation of extrasolar planets will be possible. For that purpose as well, it is necessary to need to continue studying for the realization of the FFSAT in the future.

### Acknowledgments

This paper is based on a research supported by Canon Electronics Inc. We gratefully acknowledged the support.

### References

1. Nakamura, T., “A Study on Total Serviceability Evaluation for Disaster Monitoring by Satellites (1st Report),” JOURNAL OF THE JAPAN SOCIETY FOR AERONAUTICAL AND SPACE SCIENCES, vol. 63, No. 4, pp. 143–149, 2015. (in Japanese)
2. Japan Meteorological Agency, “New geostationary meteorological satellites — Himawari-8/9 —”, <http://www.jma.go.jp/jma/>

- jma-eng/satellite/news/himawari89/himawari89\_1\_eaflet.pdf, 2014.
3. Patané, S., Fagin, M., Riley, D., Snyder, M., Kloske, J., Tobiassen, T., et al., "Precision In-Space Manufacturing for Structurally Connected Interferometry," 70th International Astronautical Congress (IAC), IAC-19,A7,3,7,x51357, 2019.
  4. Rousset, G., Mugnier, G. M., Cassaing, F., and Sorrente, B., "Imaging with Multi-aperture Optical Telescopes and an Application," C. R. Acad. Sci. Paris, srie IV, Vol. 2, No. 1, pp. 17–25, 2001.
  5. Scharf, D.P., Hadaegh, F.Y., Rahman, Z.H., Shields, J.F., Singh, G., and Wette, M.R., "An Overview of the Formation and Attitude Control System for the Terrestrial Planet Finder Interferometer," The 2nd International Symposium on Formation Flying Missions and Technologies, NASA/CP-2005-212781, 2004.
  6. Hutchison, K.D., "Applications of MODIS satellite data and products for monitoring air quality in the state of Texas," Atmospheric Environment, Vol. 37, pp. 2403–2412, 2003.
  7. Suzumoto, R., "Accurate Control of Relative Position and Attitude for Formation Flying Synthetic Aperture Telescope with Multiple Micro-satellites," 32nd International Symposium on Space Technology and Science, 2019-n-41s, 2019.
  8. Bandyopadhyay, S., Foust, R., Subramanian, G.P., Chung, S.J., and Hadaegh, F.Y., "Review of Formation Flying and Constellation Missions Using Nanosatellites," Journal of Spacecraft and Rockets, Vol. 53, No. 3, pp. 567–578, 2016.
  9. D'Amico, S., Koenig, A., Macintosh, B., and Mauro, D., "System Design of the Miniaturized Distributed Occulter/Telescope (mDOT) Science Mission," 33rd Annual AIAA/USU Conference on Small Satellites, SSC19-IV-08, 2019.
  10. Armano, M., Audley, H., Baird, J., Binetruy, P., Born, M., Bortoluzzi, D., et al., "LISA Pathfinder micronewton cold gas thrusters: In-flight characterization," Physical Review D, Vol. 99, No. 12, 122003, 2019.
  11. Smith, M.W., Donner, A., Knapp, M., Pong, C.M., Smith, C., Luu, J., et al., "On-Orbit Results and Lessons Learned from the ASTERIA Space Telescope Mission," 32nd Annual AIAA/USU Conference on Small Satellites, SSC18-I-08, 2018.
  12. Holden, B., Morgan, R., Allan, G., Pereira, P.d.V., Grunwald, W., Gubner, J., et al., "Calibration and Testing of the Deformable Mirror Demonstration Mission (DeMi) CubeSat Payload," 33rd Annual AIAA/USU Conference on Small Satellites, SSC19-WKIV-03, 2019.
  13. Miyamura, N., Suzumoto, R., Mori, D., Funabiki, N., Matsushita, S., Ikari, S., et al., "Conceptual Optical Design of a Synthetic Aperture Telescope by Small Satellite Formation Flying for GEO Remote Sensing," 32nd International Symposium on Space Technology and Science, 2019-f-59, 2019.
  14. Suzumoto, R., Ikari, S., Miyamura, N., and Nakasuka, S., "Experimental Study for  $\mu$ m-class Control of Relative Position and Attitude for Synthetic Aperture Telescope Using Formation Flying Micro-satellites," 21st IFAC World Congress, VI123.3, 2020.
  15. Gath, P.F., Fichter, W., Kersten, M., and Schleicher, A., "Drag Free and Attitude Control System Design for the LISA Pathfinder Mission," AIAA Guidance, Navigation, and Control Conference and Exhibit, AIAA 2004–5430, 2004.